

## Cysteine self-assembly on gold: A paradigm for chemisorption

O. Cavalleri and R. Rolandi\*

Department of Physics, University of Genoa, via Dodecaneso, 33, 16146 Genoa, Italy

### ABSTRACT

Pioneering studies in the early eighties demonstrated silane and alkanethiol chemisorption on oxide and gold substrates respectively. These were the first examples of coupling organic and inorganic compounds to tailor surfaces and interfaces. Technology for the new millennium will require coupling biological and inorganic systems to exploit their unique properties. Understanding the chemisorption of biological molecules on inorganic substrates will play a key role in future research endeavors. In this context, cysteine is at distinct advantage because it can bind transition metals via the native sulfhydryl group without requiring any additional chemical functionalization. The chemical reaction involved in cysteine binding to transition metals is similar to the alkanethiol self-assembly on the same substrates. However, the amino acid chirality and the presence of ionizable carboxyl and amino groups depict a particularly interesting scenario. In this paper we review cysteine chemisorption from aqueous solution or vapor on different gold surfaces. Cysteine films on gold surfaces are studied with several surface analysis techniques including infrared spectroscopy, x-ray photoelectron spectroscopy, helium scattering, metastable deexcitation spectroscopy, high resolution energy loss spectroscopy, and scanning probe microscopy. We focus this review on high resolution

photoelectron spectroscopy that is used to study the chemical status of the cysteine adsorbate. We analyze and compare the experimental results from samples solution-deposited or vapor-deposited onto Au(111) and Au(110) surfaces. X-ray photoelectron spectroscopy results are compared with the results from scanning tunneling microscopy and other investigation methods including density functional theory calculations.

**KEYWORDS:** cysteine, gold, adsorption, self-assembly, SAM, XPS, STM

### ABBREVIATIONS

AFM, Atomic Force Microscopy  
 BE, Binding Energy  
 Cys, Cysteine  
 DFT, Density Functional Theory  
 DNA, Deoxyribonucleic Acid  
 D-Cys, D-Cysteine  
 HRXPS, High Resolution X-ray Photoelectron Spectroscopy  
 IRAS, Infrared Reflection-Absorption Spectroscopy  
 L-Cys, L-Cysteine  
 NEXAFS, Near Edge X-ray Absorption Fine Structure  
 PVD, Physical Vapor Deposition  
 SAM, Self-Assembled Monolayer  
 SCE, Saturated Calomel Electrode  
 SIMS, Static Secondary Ion Mass Spectrometry  
 STM, Scanning Tunneling Microscope  
 XPS, X-ray Photoelectron Spectroscopy  
 UHV, Ultra High Vacuum

---

\*Corresponding author  
rolandi@fisica.unige.it

## INTRODUCTION

Molecules suspended in a fluid phase adhere to solid surfaces driven by intermolecular forces. At times, these molecules, activated either by thermal energy or by a non-equilibrium process such as illumination, react with the surface to form new chemical compounds bound to the solid. This phenomenon, mostly unnoticed, shapes our surroundings; common rust and fouling are formed in this fashion. For centuries, scientists have studied the adsorption of molecules on different surfaces and have learned how to exploit it. Two adsorption regimes have been identified: physisorption and chemisorption. The first one involves physical interactions with binding energies  $< 0.5$  eV per molecule ( $\sim 48$  kJ/mole) and it is only stable at low temperatures. The latter involves the formation of more stable chemical bonds and it can resist relatively high temperatures [1].

A wide majority of chemisorption studies are driven by the paramount economic interest of heterogeneous catalysis, a process widespread in multibillion dollar chemical industry. These studies mostly investigate the adsorption of inorganic molecules on metal and metal oxide surfaces with focus on the adsorbate molecules and how the surface catalytic action changes their properties. In turn, chemisorbed molecules have significant effects on the surface structure. Surface atoms can be displaced and rearranged in the chemisorption process, creating surfaces with new chemical and physical properties. Chemisorption is thus a means of tailoring material surface properties such as reactivity, wettability, friction, charge and conductivity. To this end, organic and biological molecules are more suitable than small inorganic molecules because of their increased functionality.

Since the early eighties, the interest in the chemisorption of organic molecules on inorganic surfaces has rapidly increased. Today, it is a pivotal topic in modern science and technology. Specific chemisorbed molecules are used to tailor the properties of the inorganic surface by adding specific functionalities. As such, these new designed surfaces are often referred to as "functionalized". Functionalized surfaces are used

in several technologies. Specifically, most recent analytical assays for genomics and proteomics use arrays of DNA, antibodies and proteins adsorbed in micron-sized patches onto silicon oxide. Other analytical systems use micro and nano-particles with adsorbed biomolecules [2, 3, 4, 5]. Functionalized gold nanoparticles have been proposed as drug delivery systems [6]. Chemisorbed organic molecules are used in molecular electronics and photonics [7]. Force spectroscopy and dip-pen nanolithography, two atomic force microscope techniques, rely on organic molecule chemisorption. In dip-pen nanolithography, the AFM tip is used as the nib of a pen to transfer organic inks onto suitable substrates as nanoscale patterns of chemisorbed molecules [8]. In force spectroscopy, the force between the functionalized AFM probe and the sample is measured to analyze the sample surface properties [9].

In 1980 Jacob Sagiv published a seminal paper on the absorption of silanes from organic solutions onto polar solid surfaces to produce homogenous highly-packed monolayers with controllable in plane molecular organization [10]. In this paper, Jacob Sagiv gives credit to a number of authors for having early reported, between 1947 and 1963, that the adsorption of amphipathic molecules on polar solid surfaces leads to the formation of closely packed monomolecular films with a structure similar to that of Langmuir-Blodgett monolayers deposited on solid supports from air-water interface. Three years later, Ralph G. Nuzzo and David L. Allara published a paper on the adsorption of bifunctional organic disulfides on gold surfaces [11]. In this paper, which opened the road to the study of the chemisorption of organosulfur compounds on coinage metals, the authors call "assembly" the formation process of a monolayer with extended molecular order. In the following years, this process has been often referred to as self-assembly to indicate that the organic adsorbates organize on the solid surface according to the disposition of the binding sites and molecular interactions. As a consequence, the common name for the monomolecular ordered adsorbate films is self-assembled monolayers (SAMs). In the eighties and nineties, an increasing number of papers have been published on

the chemisorption of organic molecules. Several techniques have been used to study the molecular film structure and properties, such as contact angle analysis, infrared and Raman spectroscopy, X-ray photoelectron spectroscopy, X-ray diffraction, surface second-harmonic generation, surface ionization mass spectroscopy, ellipsometry, electron and helium diffraction, surface plasmon resonance, optical microscopy, electron microscopy, scanning tunneling microscopy and atomic force microscopy. An accurate review of the first studies on SAMs can be found in Ulman's book [12].

SAMs became the samples of choice for AFM and STM studies contributing to the outset of nanoscience and nanotechnology [13]. The chemisorption of organosulphur molecules on gold attracted the most attention. Gold is a poorly reactive metal that does not oxidize at temperatures below its melting point. Gold is thus particularly suited to prepare clean surfaces in the laboratory environment. Furthermore, gold surfaces are well studied and, most importantly for nanoscience, gold easily forms thin films and colloidal particles. The most studied organosulphur compounds are alkanethiols, which are alkane molecules of different length with a thiol group (-SH) at one end (head) and a functional group at the other end (tail). Thioalkanes bind to gold, platinum, silver, and copper to form compact robust monomolecular films. The oxidation of the thiol group is responsible for bonding to the metal surface, van der Waals forces among the alkyl chain induce film packing, and the end groups provide functionality. Common end groups are carboxyls (-COOH) to form hydrophilic surfaces, and methyls (-CH<sub>3</sub>) to form hydrophobic surfaces. Many other functional groups such as biotin, cyclodextrin and calixarenes have been used to build supra-molecular architectures for molecular recognition [14]. For extensive accounts of this topic, we refer the interested reader to the reviews by Schreiber [15, 16], Zharnikov and Grunze [17], and Love *et al.* [13].

### Why cysteine?

In this paper we review the chemisorption of Cys on gold. Among organosulphur molecules Cys has a remarkably interesting self-assembly process

from the chemical and physical perspective. Cys is the only amino acid, among the 22 standard amino acids, with a free sulfhydryl group that binds to coinage metals. Sulfhydryl groups of Cys as part of proteins can be used to attach proteins and artificial peptides to metal substrates [18]. In proteins, Cys is often present in the dimeric form of cystine, formed by two cysteine residues linked by a disulfide bond. This bond is easily broken by the chemisorption on coinage metals and also cystine can act as the binding agent of proteins to metals [19, 20, 21, 22, 23]. Cys is a relatively small molecule with three functional groups, -SH, COOH, -NH<sub>2</sub> that give rise to rich interactions. The thiol group binds to metals while the carboxyl and the amino groups, besides interacting with metal surfaces, can form intramolecular hydrogen bonds. Cys can occur in four different electric states depending on the ionization of the carboxyl and the amino groups: neutral, zwitterionic, positively charged, and negatively charged. Furthermore, Cys has an asymmetric carbon atom with two chiral forms: L and D. (Fig. 1). All these features indicate that Cys molecules could have a larger number of states and configurations than alkanethiol molecules. Alkanethiol molecules only have one functional group – the thiol group – and their intermolecular interactions are limited to van der Waals forces, and steric hindrances. Another Cys feature that makes it particularly suited for research is the relatively low number of atoms that facilitates computer simulations. The large number of papers and the reliability of the information collected in about twenty years of research have made Cys chemisorption a case study in the adsorption of organic and biological molecules. We will focus this review on the chemical and physical status of Cys deposited on gold surfaces from solution and vapor. We will compare the results obtained from XPS with the results obtained from STM, IRAS and DFT calculations. In the following we will provide basic information on sample preparation and we will discuss the Cys-gold chemical reaction. Finally we will provide an outlook of this research field.

### Substrates and SAM preparation

Cys is soluble in polar solvents and SAMs can be easily prepared from solutions. For this preparation,

the substrates of choice are gold films typically prepared from PVD. The more commonly used supports are glass or mica slides and silicon wafers with a thin native oxide. Since gold does not readily form oxide, its adhesion to glass or silicon substrates is promoted with a thin film (1-5 nm) of titanium, chromium, or nickel acting as a primer. In our laboratory, freshly cleaved mica slides are often used as substrates. The evaporation is carried out at a base pressure of  $2 \cdot 10^{-6}$  mbar and the mica sheet temperature is kept at 650 K. After deposition, the films are annealed for 1–2 h in vacuum at the same temperature. Before the immersion into a Cys solution, the gold films are annealed in a butane flame until glowing red and subsequently quenched in ethanol. Flame annealing improves film structural order and cleans the surface from atmospheric adsorbates. With this procedure, polycrystalline films with atomic flat (111) terraces are prepared. These terraces are few hundred nanometers in size with the typical herringbone reconstruction of the Au(111) surface (Fig. 2a) [24, 25]. Solution-deposition can be achieved in an electrochemical cell. In this case, Cys is deposited on the working electrode at potentials higher than  $-0.42$  V (vs. SCE) and it is desorbed when the potential is scanned back to negative values [26]. The working electrodes can be made of gold films prepared as already described. Single crystal electrodes with Au(111), Au(110), and Ag(111)

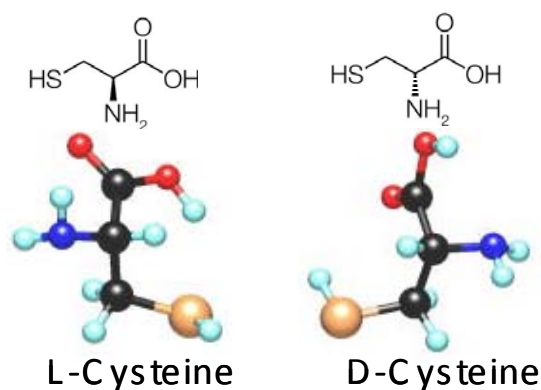


**Figure 1.** Structure formulas of the two Cys enantiomers. Color code of the sticks and balls model: black C, yellow S, red O, blue N, light blue H.

surfaces are also used especially for *in situ* STM imaging [27, 28, 29]. Cys can be deposited also from vapor phase and this method is used when measurements are performed in UHV. Cys powder is sublimated in a heated crucible (360–390 K) in an evaporation source at a background pressure of *ca.*  $10^{-10}$  mbar [30, 31]. For UHV measurements, gold single crystals cleaned by 1–1.5 keV  $\text{Ar}^+$  sputtering and annealing at about 800 K are usually used.

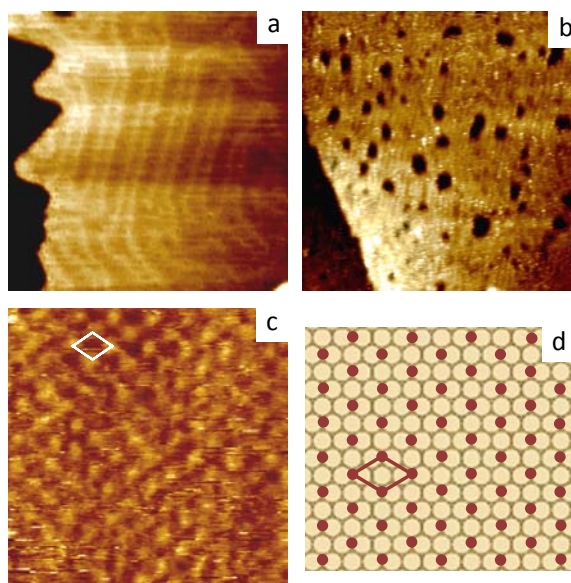
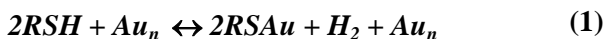


**Figure 2.** (a) STM image of the gold substrate showing the  $(22 \times \sqrt{3})$  reconstruction of the Au(111) surface. Image size  $55 \times 55$  nm. Tunneling parameters:  $I = 5.0$  nA,  $V = 10$  mV. (b) STM image of a L-Cys-covered Au(111) surface. The dark spots are nm-size, one gold atom deep, depressions, commonly observed in gold surfaces after the deposition of organosulphurs. Image size  $90 \times 90$  nm. Tunneling parameters  $I = 0.8$  nA,  $V = 100$  mV. (c) Molecular resolution STM image of the L-Cys adsorbate on Au(111). The Fourier transform analysis of several molecular resolution images provided that the nearest neighbor distance in the hexagonal lattice is  $(0.49 \pm 0.01)$  nm compatible with the formation of a  $(\sqrt{3} \times \sqrt{3})$  R30° adlayer. (d) Coverage scheme of L-Cys chemisorbed on Au(111). Yellow balls represent gold atoms. Brown ball represents L-Cys molecules bonded at bridge sites. The parallelogram is a guide for comparing these scheme with the pattern of the image in the panel c. Panels a, b, c are reprinted from Dodero, G. *et al.*, 2000, *Colloids Surf. A*, 175, 121 with permission from Elsevier.

### Binding reaction

Organosulphur compounds are adsorbed on gold as thiolates, according to the reaction:



where  $R$  is the organic moiety of the organosulphur compound and  $Au_n$  represents the gold surface atoms. In the case of Cys,  $R$  is



We assume that the proton of the sulfhydryl group is lost as molecular hydrogen. Another potential route for the proton is to form gold hydride. However, this case is less probable as indicated by DFT calculations [32].

The binding reaction can proceed if the thiol group is activated. The details of the activation process and sulfur oxidation are still elusive. Specifically, it is not clearly determined what happens to the hydrogen of the  $-SH$  group. Love *et al.* advance the hypothesis for alkanethiols that, in vacuum, the hydrogen may be eliminated as molecular hydrogen, while, in solution, the oxygen may induce oxidative conversion of the hydrogen to water [13]. The precise energetics of this reaction is also not fully determined. Thermally activated desorption studies by Lavrich *et al.* yield an alkanethiol desorption energy in vacuum of 126 kJ/mole with an activation energy of about 28.8 kJ/mole [33]. Both these energies are independent of the length of the alkyl chain. Recently, these values have been confirmed by the DFT calculations of Tielens and Santos [32]. These authors calculate that S-H bond breaking requires an activation energy of about 31 kJ/mole, while the formation enthalpy of Au-S bond formed by the thiolate radical is in the range of  $-115$  and  $-125$  kJ/mole depending on the binding site. Furthermore, they found that the production of  $H_2$  is more favorable than the formation of Au-H species. For the chemisorption of alkanethiols on gold from solution with the production of molecular hydrogen Schlenoff *et al.* measure an adsorption enthalpy of  $-23$  kJ/mole [34]. The differences of the chemisorption processes in vacuum and in solution explains the large discrepancy between the Schlenoff value and that measured by Lavrich *et al.* and confirmed by the

DFT calculations of Tielens and Santos. In the presence of the solvent, the dissolution enthalpy of the adsorbate and that of the substrate immersion must be taken into account. A detailed comparison of the adsorption energies involved in vapor-adsorption and solution-adsorption has not yet been performed.

To the best of our knowledge, there are no values for Cys binding energy obtained from experimental measurements. A few values have been calculated with DFT calculations. Nazmutdinov *et al.* [35] perform DFT computations to obtain the optimized geometry for the adsorption of four L-Cys forms: the molecule, the radical ( $S-CH_2-CH(NH_2)-COOH$ ), its zwitterion form ( $S-CH_2-CH(NH_3^+)-COO^-$ ), and the cysteinate anion ( $-S-CH_2-CH(NH_2)-COOH$ ). These forms are adsorbed with different orientations at the top, bridge, and threefold hollow sites of a planar Au(111). In their paper the adsorption energy  $\Delta E_{ads}$ , is calculated as:

$$\Delta E_{ads} = E_{tot}(Au_n - Cys) - E_{tot}(Au_n) - E_{tot}(Cys) \quad (2)$$

where  $E_{tot}(Au_n - Cys)$  is the total energy of the system with Cys bonded to gold, and  $E_{tot}(Au_n)$  and  $E_{tot}(Cys)$  are the total energies of the cluster made of  $n$  gold atoms and one molecule of the different Cys forms, respectively. For Cys adsorbed from gas phase, Nazmutdinov and coworkers obtain values (for different adsorption sites and the different Cys orientations) that range between  $-60$  kJ/mole for zwitterions Cys in a hollow site and  $-240$  kJ/mole for anion Cys in a hollow site. A similar calculation is performed by Santos and coworkers for Cys adsorbed from gas phase on Ag (111) [29]. The reported values range between  $-96$  kJ/mole for radical Cys in a top site and around  $-221$  kJ/mole for zwitterions Cys in different sites. In this paper the authors also reduce the data reported by Di Felice and coworkers to the adsorption energy defined in eq. 2. These values are  $-196$  kJ/mole and  $-162$  kJ/mole for radical Cys adsorbed from gas phase at the bridge site and at the hollow site respectively [36, 37]. Nazmutdinov and coworkers also compute the ‘‘desolvation energy’’, which is the free energy change when a particle from the bulk approaches the interface. The computed

values range from  $-11.3$  kJ/mole for radical Cys and  $-77.3$  kJ/mole for anion Cys [35].

### Chemisorption from solution

In one of the first papers on the chemisorption of Cys on polycrystalline gold films from solution, Ihs and Liedberg report that L-Cys forms an adsorbate bound to the gold surface through the thiol group, as indicated by IRAS measurements. L-Cys is in a non-zwitterionic form when deposited from an aqueous solution at pH 1.5 and 5.7, while its carboxyl group is ionized when deposited at pH 11.7 [38]. In a subsequent paper, the same Linköping research group reports on an XPS-based study of L-Cys deposited on polycrystalline gold and copper surfaces by vapor deposition and solution [39]. By comparing the XPS results for adsorbates prepared from vapor deposition and from solution (pH  $5.7 \pm 0.3$ ), the authors observe that in both the cases the L-Cys adsorbate is about 0.5 nm thick and that about one-half of the sulfur atoms are bonded to the metal surface. On these bases, the authors propose that L-Cys on gold forms a bimolecular film with the first molecular layer covalently bound to gold, and the second layer physisorbed onto the first. Furthermore, they observe that, in the films prepared from solution, some of the amino groups change from  $-\text{NH}_3^+$  to  $-\text{NH}_2$  and only very few of the  $-\text{NH}_2$  groups are localized close to the gold surface. In 1993, Leggett *et al.*, reported from SIMS measurements that, in the L-Cys adsorbate, the sulfur-gold bond is as strong as that the dominant fragmentation steps involve the scission of the S-C bond and ejection of gold atoms bound to fragments of L-Cys molecules [40].

In one of the first studies on the electrochemical deposition of L-Cys on a Au(111) electrode, Dakkouri and coworkers report images obtained by *in situ* STM, that is, without removing the sample from the electrochemical cell. *In situ* electrochemical STM is performed by using an insulated tip with a conducting apex. Usually the tip potential is controlled independently from the potential of the working electrode. These images demonstrate that L-Cys adsorption began at a potential of  $-0.40\text{V}$  vs. SCE. At this potential the  $(22 \times \sqrt{3})$  herringbone reconstruction of the Au(111) surface is lifted. At more positive potentials,

L-Cys forms a hexagonal pattern with a nearest-neighbor distance of  $(0.49 \pm 0.02)$  nm in agreement with a  $(\sqrt{3} \times \sqrt{3})$  R30° adlayer structure. Scanning back the potential to negative values causes Cys desorption and leaves the electrode surface roughened by a large number of one-atom deep holes [26].

These findings are confirmed for deposition of L-Cys without electrochemical control. Dodero *et al.*, report on L-Cys deposited on multi-crystalline Au(111) surfaces from solution [24]. In their paper, which was presented at the 1st International Conference on Amphiphiles at Interfaces, held in Beijing in 1999, the main chemical and structural features of L-Cys adsorbed on Au(111) from XPS and STM measurements are put together. STM images obtained in air show that L-Cys adsorption results in the lifting of the  $(22 \times \sqrt{3})$  herringbone reconstruction accompanied by the formation of depressions that are a few nm wide and one atomic layer deep (Fig 2, a, b, and c). This suggests that the L-Cys chemisorption process in solution is spontaneous and very similar to the alkanethiol chemisorption process [13]. It is commonly accepted that these depressions are caused by the removal of adsorbed molecules still bound to gold atoms as indicated by electrochemistry and SIMS measurements [26, 40]. STM and AFM imaging shows that these depressions are eventually covered by adsorbate molecules [41]. Molecular resolution STM images confirm the formation of an ordered L-Cys adlayer with a hexagonal lattice. The nearest-neighbor distance in this lattice is found to be  $(0.49 \pm 0.01)$  nm, compatible with a  $(\sqrt{3} \times \sqrt{3})$  R30° adlayer and in complete agreement with the value measured by *in situ* STM by Dakkouri and coworkers [26]. This structure is formed by one molecule of L-cysteine every three gold atoms. This 1 to 3 balance is in good agreement with the coverage of chemisorbed L-Cys evaluated from XPS measurements.

The formation of a strong covalent bond between Cys and gold observed by Linköping group [38, 39] is confirmed by the analysis of the XPS results in the region of the S2p core level. The spectrum of the S2p core level is characterized by a doublet corresponding to the  $2p_{3/2}$  and  $2p_{1/2}$

splitting induced by spin-orbit interaction. The energy separation (1.2 eV) and the intensity ratio (2:1) of the doublet peaks are the same for different sulfur species, but the peak position depends on the sulfur chemical species. Conventionally the doublet position is identified by the position of the larger  $2p_{3/2}$  component. Dodero and coworkers report the presence of two sulfur species similarly to Uvdal and coworkers [24, 39]. The most abundant one is sulfur in thiolate groups with the doublet at BE of 162.2 eV. The less abundant, at BE of 164.1 eV, is attributed to sulfur weakly bound to gold surface, probably thiol group sulfur of physisorbed L-Cys. Interestingly, the N1s region of the spectrum shows the presence of two nitrogen species, the one with BE of 399.6 eV is attributed to the nitrogen in the  $\text{NH}_2$  groups, the other one, with BE of 401.7 eV is attributed to the nitrogen of  $\text{NH}_3^+$  groups. These findings suggest that some of L-Cys molecules are in zwitterion form. The low resolution of their XPS measurements did not allow the authors to confirm this observation by the results of the carbon core level spectrum.

To clarify the L-Cys ionization state and the existence of a layer physisorbed onto the chemisorbed one, the authors of this paper, with their coworkers at Genoa University, carried out synchrotron radiation-based HRXPS measurements on L-Cys solution-deposited on polycrystalline Au(111) [42]. Fig. 3 shows typical results of those measurements on pristine SAMs of purified L-Cys. In the spectral region of the S2p core level (Fig. 3a) the photoelectron spectrum shows two prominent peaks representative of the  $2p_{3/2}$  and  $2p_{1/2}$  splitting. A small shoulder, around 161 eV BE, indicates the presence of two different sulfur species. The main doublet ( $S_A$  species) occurs at 161.9 eV BE. The less intense doublet ( $S_B$  species), is at 161.2 eV BE. The dominant  $S_A$  state coincides, within experimental uncertainty, with the previously observed thiolate species produced by the chemical reaction of L-Cys with Au. Control measurements on samples prepared with non-recrystallized L-Cys, and on pre-irradiated heated samples indicate that the  $S_B$  species is atomic sulfur either present as contaminant in the preparation materials or produced by SAM damage. Interestingly, the sulfur state with the BE

of about 164 eV, identified as the sulfur in the thiol groups of physisorbed Cys molecules, which was previously observed by both Linköping and Genoa groups [38, 39 and 24], is not present. This state seems to be present, with intensity much lower than the  $S_A$  signal, as a result of a poor rinsing procedure. The first important clarification from HRXPS measurements is that the L-Cys chemisorption from solution produces a monomolecular film covalently bound to the gold surface [42, 43].

In the N1s core level spectral region (Fig. 3b), the signal has two peaks, best reproduced by the sum of two pseudo-Voigt functions. The main peak ( $N_A$ ), is centered at 401.4 eV, whereas, the other ( $N_B$ ) is located at 399.4 eV.  $N_A$  and  $N_B$  are assigned to protonated amine nitrogen ( $-\text{NH}_3^+$ ) and amine nitrogen ( $-\text{NH}_2$ ), respectively. The C 1s spectral region signal also shows two peaks, but each one has a shoulder on the high BE side (Fig. 3c). The deconvolution procedure reveals four maxima at 284.6 eV ( $C_A$ ), 286.0 eV ( $C_B$ ), 287.7 eV ( $C_C$ ), and 288.9 eV ( $C_D$ ), corresponding to four carbon species.  $C_A$  is assigned to adventitious hydrocarbons ( $-\text{CH}_2-$ ) and carbon bonded to sulfur ( $-\text{H}_2\text{CS}-$ ).  $C_B$  is assigned to carbon bonded to nitrogen ( $-\text{CN}-$ ).  $C_C$  and  $C_D$ , are assigned to carboxylate carbon ( $-\text{COO}-$ ) and carboxyl carbon ( $-\text{COOH}$ ), respectively. In the O1s core level region, the signal is characterized by a broad, asymmetric peak with a marked shoulder on the high BE side (Fig. 3d). Also in this case, the authors cannot rule out that part of the signal is due to adventitious oxygen. The best-fit procedure allowed the authors to identify three oxygen species:  $O_A$  is carbonyl ( $-\text{C}=\text{O}$ ) oxygen,  $O_B$  is ionized oxygen in carboxylate ( $-\text{COO}^-$ ),  $O_C$  is hydroxyl ( $-\text{COOH}$ ) oxygen. The presence of adventitious oxygen did not allow a complete quantitative analysis of the different species, but the analysis of the carbon and nitrogen signals strongly suggested the presence of both zwitterionic and undissociate L-Cys in the adsorbate layer. The evaluation of the amount of the different chemical species suggested that there are three zwitterions for each neutral molecule. This ratio does not mirror that one in the adsorption solution at pH 5.7, in which the zwitterion form is by far dominant. Since XPS

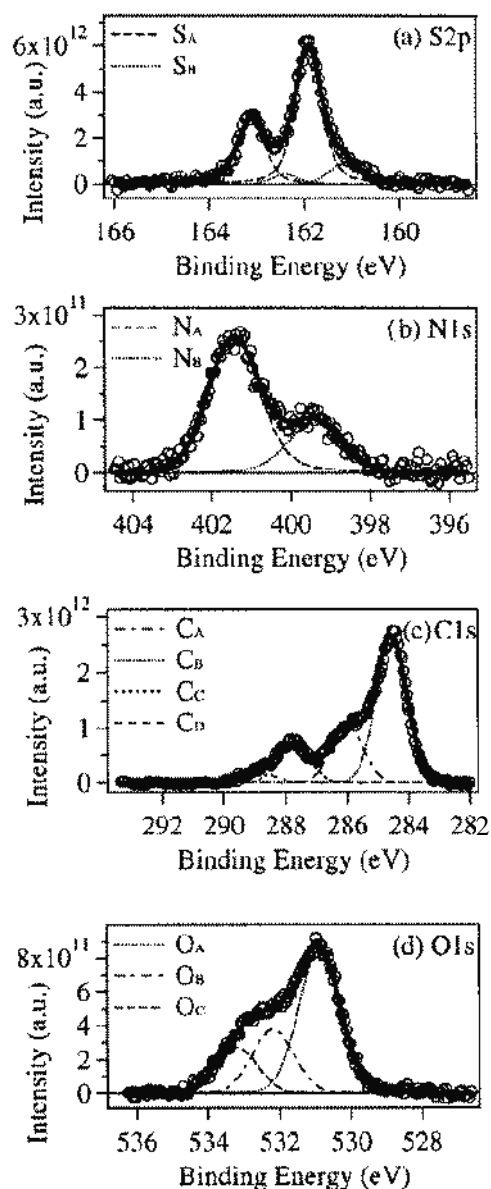


**Figure 3.** High resolution X-ray photoelectron spectra of pristine Cys SAMs prepared by solution-deposition. (a) S2p core level region, photon energy: 270 eV. (b) N1s core level region, photon energy: 690 eV. (c) C1s core level region, photon energy: 690 eV. (d) O1s core level region, photon energy 690 eV. The open circles are the experimental data after background subtraction. The continuous thick lines represent the best fits to the experimental data of the sum of pseudo-Voigt functions. Each pseudo-Voigt function represents the contribution of a chemical species to the signal. The thin continuous and dashed lines are the resolved components contributing to the signal. [Cavalleri, O. *et al.*, 2004, Phys. Chem. Chem. Phys., 6, 4042] - Reproduced by permission of the PCCP Owner Societies.

measurements are performed on dry samples, this fact strongly suggests that charge redistribution occurs either in the chemisorption process or in the drying process.

Strong environmental effects are confirmed by *in situ* STM imaging of electrochemically deposited Cys. Different adlayer structures have been observed in different solutions: close packing ( $\sqrt{3} \times \sqrt{3}$ ) R30° in the presence of H<sub>2</sub>SO<sub>4</sub> [26], ( $3\sqrt{3} \times 6$ ) R30° in NH<sub>4</sub>Ac at pH 4.6 [27] and ( $4 \times \sqrt{7}$ ) R19° in HClO<sub>4</sub> [44] have been observed on Au (111). How solutes and solvents affect adlayer structure has not been clarified until now.

Zhang and coworkers observe a  $c(2 \times 2)$  lattice on Au(110) in NH<sub>4</sub>Ac at pH 4.6 [28]. The STM images presented in their paper have sub-molecular resolution and the authors are able to delineate the main factors that determine electronic contrasts in the STM images by using model DFT calculations. These factors include molecular orientation, chemical nature of molecular elements or groups, and element interaction with tip and substrate. The computational images recast as constant-current-height profiles show that the most favorable molecular orientation is the adsorption of Cys as a radical in zwitterion form located on the bridge between the Au(110) atomic rows and with the amine and carboxyl group toward the solution bulk. The submolecular features observed in solution are different from those observed in ultrahigh-vacuum (*vide infra*). This strengthens the conjecture that the solvent plays an important role during molecular assembly.

### Chemisorption from vapor phase

For many practical aspects, SAM deposition from solution is very convenient. However, this preparation method often involves unwanted contamination from solution and lab atmosphere as we have observed with HRXPS. Even using non reactive substrates, such as gold, does not assure the absolute cleanliness of the surface. In many cases, the strength of the chemisorption reaction is sufficient to remove weakly-adsorbed contaminants, but adventitious species can be adsorbed onto the SAM during the following sample handling. For this reason, preparations and

measurements performed in UHV without exposing the samples to gas and liquid environment are often preferred. In the case of Cys SAMs, the comparison between the results of chemical and structural analysis of SAMs prepared from solution and in UHV clarifies the role of the environment in determining the SAM structure.

Uvdal *et al.* vapor-deposited L-Cys on multi-crystalline gold and copper surfaces in a preparation chamber connected to a XPS spectrometer [39]. Both copper and gold substrates had a preferred (111) crystalline orientation. The measurements were performed on films thicker than 4 nm and thin adsorbates kept at 223 K. In their paper, by analyzing C1s, O1s, N1s and S2p core level spectra these authors conclude that, in thick films, L-Cys is in the zwitterionic state with an unchanged thiol group, as observed in Cys powder. In adsorbates, both chemisorbed and physisorbed L-Cys is present. Their adsorbate spectra in the S2p region show two separate doublets: one at 161.9 eV for thiolate species, the other at 164.0 eV close to the doublet position observed in thick films. From peak relative intensities, the authors deduce that, in the adsorbate, almost 50% of the sulfur is bonded to the gold. They do not observe any significant difference between thick films and adsorbates in the regions of N1s and O1s core levels. On the basis of these findings and of the value of adsorbate thickness (0.6 nm) the authors propose that the adsorbate is made of a double layer of molecules with the second layer that partially overlaps the first.

The paper of De Renzi *et al.* confirms the contemporary presence of physisorbed and chemisorbed molecules in L-Cys layers vapor-deposited on Au(111) [45]. These authors provide a refined interpretation of the vapor deposition process on the basis of HRXPS and HREELS measurements performed at different coverages. They demonstrate that room-temperature deposition of L-Cys leads to heterogeneous adsorbed chemical species. At low coverage (0.2 ML) only the chemisorbed species is detected. Increasing the coverage the physisorbed component increases and it becomes the predominant species at 1ML. These findings suggest that, at room temperature,

L-Cys initially is chemisorbed at steps and defects, then it is physisorbed on terraces. At higher temperature (330 K), a homogenous monolayer made of chemisorbed zwitterionic molecules interacting through a well-organized H-bond network is formed.

UHV STM imaging confirms this scenario only in part. Kühnle *et al.* [31], on Au(111), at room temperature and at low coverage, observe irregular molecular islands of L-Cys molecules on gold terraces. At higher coverage, these islands grow in size and ordered patches with square symmetry appear. In these conditions, typical herringbone reconstruction is clearly visible underneath the Cys layer indicating that Cys molecules are physisorbed. Only after annealing to 380 K the herringbone reconstruction is perturbed and, at high coverage, the  $(\sqrt{3}\times\sqrt{3})$  R30° overlayer appears. In contrast with the results of HRXPS measurements, STM imaging does not detect chemisorbed molecules at room temperature. We note that spectroscopic and microscopy techniques cover different spatial ranges. Microscopes, and in particular scanning probe microscopes, explore selected areas of the sample. Therefore they can either point out or neglect minority features of the sample.

In conclusion, Cys vapor-deposited on Au(111) at room temperature forms a layer in which the molecules are physisorbed on terraces. Chemisorbed molecules can be present on the most reactive sites (steps and defects).

A slightly different scenario appears considering L-Cys adsorption on Au(110). The Genoa group performed HRXPS and HREED on L-Cys vapor deposited on Au (110) at room temperature with different degree of coverage (from sub-monolayer to one layer) [30]. The HRXPS results of the S2p, C1s, N1s and O1s core level spectra are shown in Figure 4, 5 and 6. The S2p region (Fig. 4) is characterized by a well-defined doublet, S1, at  $(161.95 \pm 0.05)$  eV. This doublet coincides with the  $S_A$  signal of Fig. 3a and indicates the formation of a thiolate compound. Thiolate sulfur is the only sulfur species in the sample until complete coverage is reached (spectrum e). To better describe this last spectrum, an additional doublet has been added in the 164-166 eV region. As it was demonstrated by control measurements on

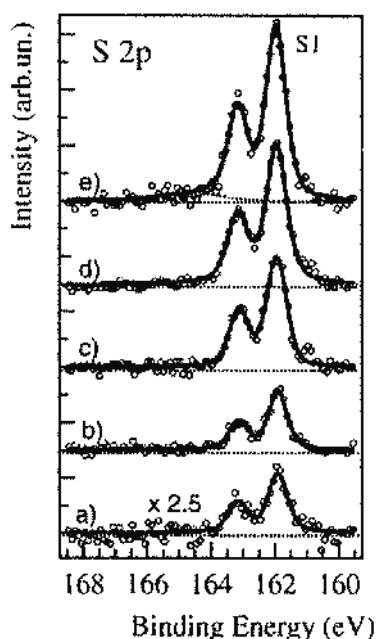


**Figure 4.** High resolution X-ray photoelectron spectra obtained in the S2p core level region as a function of coverage in the submonolayer adsorption regime, photon energy 710 eV, (a) 0.14 (b) 0.33 (c) 0.62 (d) 0.8, and (e) 1 ML. Circles: experimental data after normalization to the photon beam flux and background subtraction. Continuous lines are the best fit to the experimental data of the sum of the pseudo-Voigt functions representing the deconvoluted components of the signal. Reprinted with permission from Ref. [30]. Copyright 2005 American Chemical Society.

thicker L-Cys films, this signal indicates the initial formation of a new physisorbed layer. Physisorbed layers characterized by the doublet at  $(164.3 \pm 0.1)$  eV were removed by mild annealing up to 373 K. In the C1s region (Figure 5), four peaks, C1 at  $(284.8 \pm 0.1)$  eV, C2 at  $(286.3 \pm 0.1)$  eV, C3 at  $(288.2 \pm 0.1)$  eV and C4 at  $(289.2 \pm 0.1)$  eV are necessary to reproduce the whole set of data consistently. There is a correspondence between these four peaks and those in Fig. 3c, but in this case the presence of adventitious carbon can be ruled out. C1 and C2 are assigned to  $C_{\beta}$  ( $\text{HSC}_{\beta}\text{H}_2\text{CH}(\text{NH}_2)\text{COOH}$ ) and  $C_{\alpha}$  atoms ( $\text{HSCH}_2\text{C}_{\alpha}\text{H}(\text{NH}_2)\text{COOH}$ ), respectively. The C3 and C4 signals fall in the energy region typical of carboxyl. In the N1s region (panel A in Figure 6), two relatively broad peaks were resolved, N1 at  $(399.5 \pm 0.2)$  eV and N2 at  $(401.5 \pm 0.2)$  eV. These peaks that coincide with those of Figure 3b

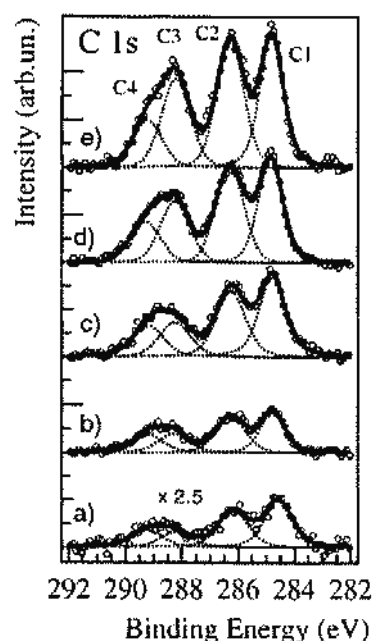


**Figure 5.** Same as for Figure 4, but for the C1s core level region. Circles: experimental data after normalization to the photon beam flux and background subtraction. Continuous lines: best fit. Dottedlines: deconvolution with pseudo-Voigt peaks. Reprinted with permission from Ref. [30]. Copyright 2005 American Chemical Society.

indicate the presence of  $-\text{NH}_2$  and  $-\text{NH}_3^+$  groups. The O1s spectra (panel B) exhibit a broad structure, related to oxygen atoms belonging to  $\text{COOH}$  and  $\text{COO}^-$  groups. This signal was deconvoluted in three peaks O1 at  $(531.2 \pm 0.1)$  eV, O2 at  $(532.3 \pm 0.2)$  eV, and O3 at  $(533.6 \pm 0.2)$  eV BE. Also in this case the presence of adventitious oxygen can be ruled out and there is a correspondence between these results and those reported in Fig. 3d. Therefore O1 is carbonyl ( $-\text{C}=\text{O}$ ) oxygen, O2 is ionized oxygen in carboxylate ( $-\text{COO}^-$ ), and O3 is hydroxyl ( $-\text{COOH}$ ) oxygen. Interestingly, the relative intensities of C3 and C4, N1 and N2, and O1, O2 and O3 change as the coverage increases. Specifically, N1 reaches saturation intensity while N2 continues to increase for depositions up to 1 ML and beyond. At low coverage, the neutral acidic fraction ( $\text{AuSCH}_2\text{-CH}(\text{NH}_2)\text{COOH}$ ) is most abundant with the possible occurrence of molecules with cationic character ( $\text{AuSCH}_2\text{CH}(\text{NH}_3^+)\text{COOH}$ ), while, as coverage

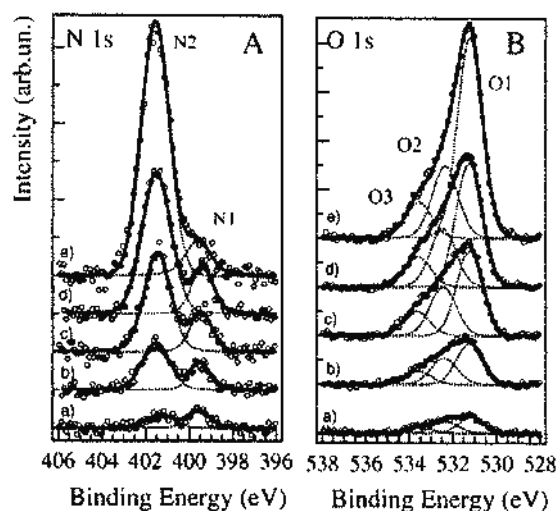


**Figure 6.** Same as Figures 4 and 5 but for the (A) N1s and (B) O1s core level regions. Circles: experimental data after normalization to the photon beam flux and background subtraction. Continuous lines: best fit. Dotted lines: deconvolution with pseudo-Voigt peaks. Reprinted with permission from Ref. [30]. Copyright 2005 American Chemical Society.

approaches the monolayer limit and beyond, the population weight of the zwitterionic species ( $\text{AuSCH}_2\text{CH}(\text{NH}_3^+)\text{COO}^-$ ) fraction increases and becomes the main one.

Moving from the described results, Cossaro *et al.* [46] used NEXAFS and in-plane XRD measurements, at different coverage, to track the L-cysteine domain grown on Au(110). These authors report the formation of molecule rows along the  $[1\bar{1}0]$  direction at room temperature accompanied by the removal of the missing row gold reconstruction. The molecular rows are always coupled in pairs yielding a quasi-fourfold periodicity along the  $[001]$  direction. According to the author model, the rows are formed by zwitterionic molecules. Each molecule has the  $\text{COO}^-$  group aligned to the  $\text{NH}_3^+$  group of the consecutive molecule in the same row and facing the  $\text{NH}_3^+$  group of a molecule in the adjacent row. This picture is consistent with the STM images obtained by Kühnle and coworkers [47, 48] and with *in situ* electrochemical STM images and DFT calculations by Zhang *et al.* [28].

HRXPS measurements on vapor-deposited L-Cys on Au(110) indicate that L-Cys is chemisorbed at

room temperature and that, on the contrary of what happens with Au(111), no physisorbed L-Cys is detected up to the 1 ML coverage [30]. Also in this case the scenario is in part confirmed by UHV STM imaging. The Aarhus group performed a series of UHV STM-based studies on Cys vapor-adsorbed on Au(110) [47, 48, 49, 50, 51]. In the first of these works, Kühnle *et al.* [49] report on the formation of Cys dimers that cannot be moved by the STM tip at room temperature. In a subsequent paper [50] the same group describes the formation of irregular islands when Cys is deposited at 120 K. Annealing to 270 K induces the formation of clusters composed of eight molecules. These clusters, at 260 K, are moved by the STM tip along the  $[1\bar{1}0]$  direction, leaving behind an unperturbed gold surface. This indicates that the clusters are physisorbed rather than chemisorbed to the substrate. The transition from physisorbed Cys to chemisorbed cysteinate was observed after annealing to 340-380 K. At low coverage, Cys dimers that cannot be manipulated are formed in parallel with gold surface restructuring. With increasing coverage, double rows along the  $[1\bar{1}0]$  direction are formed. These rows are consistent with those detected by XRD [46] and observed by *in situ* electrochemical STM [28]. These observations suggest that, on Au(110), Cys is chemisorbed at temperatures around room temperature.

In this review we focus the attention on chemisorption process and do not discuss the overlayer order as a function of substrate conditions, and adsorbate chemical status. In our opinion, this subject deserves further investigation after the intriguing scenario outlined by the Aarhus group in their work [51]. In three important papers, Besenbacher and coworkers demonstrate the chiral recognition of Cys molecules forming clusters [49, 50, 48]. Specifically, these authors show that dimers formed at low coverage on Au(110) by a racemic mixture of Cys are exclusively homochiral [49]. When clusters of molecules are formed, those formed by L-Cys have a mirror symmetry with respect to those formed by D-Cys [50]. Furthermore, L-dimers are rotated of  $20^\circ$  clockwise with respect to close packed  $[1\bar{1}0]$  direction, while D-dimers are rotated anticlockwise by the same angle.

L-dimers and D-dimers form different angles when adsorbed at S kink sites. These dimers seem to act as nucleation sites for islands of homochiral molecules. Islands of D-Cys preferentially grow from S kinks, while those of L-Cys preferentially grow from R kinks [48].

## FINAL REMARKS

Cys chemisorption is part of the rapidly growing field of molecular self-assembly on surfaces. The adsorption of this amino acid on coinage metals and in particular on gold has become a widely studied subject. With the aid of spectroscopic studies and advanced microscopy, Cys chemisorption has become almost as main stream as alkanethiols on gold. However, Cys molecular complexity makes Cys adsorbate a significantly richer system with several unique features. Among these, there is the role played by the deposition procedure. In solvent-deposition, the solution pH determines the chemical state of the adsorbate; *in situ* STM has revealed different overlayer textures for different bathing solutions. For chemisorption in vacuum, interestingly, different behaviors are observed for Au(111) and A(110). HRXPS and HREELS indicate that on Au(111), at room temperature, chemisorption occurs together with physisorption. The first probably occurs at steps and defects. In this case, STM imaging detects only physisorbed molecules on terraces. We advance the hypothesis that the local nature of the scanning probe microscopy is responsible for this result. Probably a temperature threshold for chemisorption does not exist and chemisorbed molecules can coexist with physisorbed ones in a wide temperature range. Temperature affects the numerical ratio between physisorbed molecules and chemisorbed ones. The different reactivities of different surface sites justify the coexistence of the two populations and the confinement of chemisorbed molecules at more reactive sites.

For Au(110) both spectroscopic and STM results agree in indicating that, around room temperature Cys is chemisorbed. The recognized higher reactivity of the (110) surface justifies this finding.

The physical chemistry of the Cys chemisorption still has many unanswered questions. One of these

questions is the role of molecular diffusion and molecular interaction prior to chemisorption. Another question is the role of the H-bond network in determining the overlayer structure. Perhaps a more interesting and more challenging future endeavor is to develop the use of Cys chemisorption in practical applications. We have seen that Cys can already be used to bind polypeptides and proteins to metallic surfaces for the preparation of selective electrodes. Cys unique properties could suggest more refined and appealing uses.

## ACKNOWLEDGMENTS

We would like to thank Prof. M. Canepa, for his stimulating and constructive criticism and his precious collaboration in the Cys project and Prof. M. Rolandi (University of Washington, Seattle) for critical revisions of the manuscript.

The Cys project has been extending for several years and it has been funded by CNR, Genoa University, MIUR and INFM.

## REFERENCES

1. Norskov, J. K. 1990, Rep. Prog. Phys., 53, 1253.
2. Sassolas, A., Leca-Bouvier, B. D., and Blum, L. J. 2008, Chem. Rev., 108, 109.
3. Yu, X. B., Schneiderhan-Marra, N., and Joos, T. O. 2010, Clinical Chemistry, 56, 376.
4. Rosi, N. L. and Mirkin, C. A. 2005, Chem. Rev., 105, 1547.
5. Barbulovic-Nad, I., Lucente, M., Sun Y., Mingjun Zhang M., Wheeler, A. R., and Bussmann M. 2006, Critical Reviews in Biotechnology, 26, 237.
6. Arvizo, R., Bhattacharya, R., and Mukherjee, P. 2010, Expert Opinion on Drug Delivery, 7, 753.
7. Astruc, D., Boisselier, E., and Ornelas, C. 2010, Chem. Rev., 110, 1857.
8. Piner, R. D., Zhu, J., Xu, F., Hong, S. H., and Mirkin C. A. 1999, Science, 283, 661.
9. Goeders, K. M., Colton, J. S., and Bottomley, L. A. 2008, Chem. Rev., 108, 522.
10. Sagiv, J., 1980, J. Am. Chem. Soc., 102, 92.
11. Nuzzo, R. G. and Allara, D. L. 1983, J. Am. Chem. Soc., 105, 4481.

12. Ulman, A. 1991, *An Introduction to Ultrathin Organic Films, from Langmuir-Blodgett to Self-Assembly*, Academic Press Inc., Boston.
13. Love, J. C., Estroff, L. A., Kriebel, J. K., Nuzzo, R. G., and Whitesides G. M. 2005, *Chem. Rev.*, 105, 1103.
14. Ludden, M. J. W., Reinhoudt, D. N., and Huskens, J. 2006, *Chem. Soc. Rev.*, 35, 1122.
15. Schreiber, F. 2000, *Progress in Surface Science*, 65, 151.
16. Schreiber, F. 2004, *J. Phys.: Condens. Matter*, 16, R881.
17. Zharnikov, M. and Grunze M. 2001, *J. Phys.: Condens. Matter*, 13, 11333.
18. Sasaki, Y. C., Yasuda, K., Suzuki, Y., Ishibashi, T., Sato, I., Fujiki, Y., and Ishiwata S. 1997, *Biophysical J.*, 72, 1842.
19. Zhang, H. M., Li, Y., Xu X., Sun, T. L., Fuchs, H., and Chi, L. F. 2010, *Langmuir*, 26, 7343.
20. Bordi, F., Prato, M., Cavalleri, O., Cametti, C., Canepa, M., and Gliozzi, A. 2004, *J. Phys. Chem.*, 108, 20263.
21. Chi, Q. J., Zhang J. D., Nielsen, J. U., Friis, E. P., Chorkendorff, I., Canters, G. W., Andersen, J. E. T., and Ulstrup, J. 2000, *J. Am. Chem. Soc.*, 122, 4047.
22. Andolfi, L., Bruce, D., Cannistraro, S., Canters G. W., Davis J. J., Hill, H. A. O., Crozier, J., Verbeet, M. P., Wrathmell, C. L., and Astier, Y. 2004, *Journal of Electroanalytical Chemistry*, 565, 21.
23. Cavalleri, O., Natale, C., Stroppolo, M. E., Relini, A., Cosulich, E., Thea, S., Novi, M., and Gliozzi, A. 2000, *Phys. Chem. Chem. Phys.*, 2, 4630.
24. Dodero, G., De Michieli, L., , Cavalleri, O., Rolandi, R., Oliveri, L., Dacca, A., and Parodi, R. 2000, *Colloids Surf. A*, 175, 121.
25. Cavalleri, O., Oliveri, L., Dacca, A., Parodi, R., and Rolandi, R. 2001, *Appl. Surf. Sci.*, 175-176, 357.
26. Dakkouri, A. S., Kolb, D. M., Edelstein-Shima, R., and Mandler, D. 1996, *Langmuir*, 12, 2849.
27. Zhang, J., Chi, Q. J., Nielsen, J. U., Friis, E. P., Andersen, J. E. T., and Ulstrup, J. 2000, *Langmuir*, 16, 7229.
28. Zhang, J. D., Chi, Q. J., Nazmutdinov, R. R., Zinkicheva, T. T., and Bronshtein, M. D. 2009, *Langmuir*, 25, 2232.
29. Santos, E., Avalle, L., Pötting, K., Vélez, P., and Jones, H., 2008, *Electrochimica Acta*, 53, 6807.
30. Gonella, G., Terreni, S., Cvetko, D., Cossaro, A., Mattera, L., Cavalleri, O., Rolandi, R., Morgante, A., Floreano, L., and Canepa, M. 2005, *J. Phys. Chem. B*, 109, 18003.
31. Kühnle, A., Linderoth, T. R., Schunack, M., and Besenbacher, F. 2006, *Langmuir*, 22, 2156.
32. Tielens, F. and Santos, E. 2010, *J. Phys. Chem. C*, 114, 9444.
33. Lavrich, D. J., Wetterer, S. M., Bernasek, S. L., and Scoles, G. 1998, *J. Phys. Chem. B*, 102, 3456.
34. Schlenoff, J. B., Li, M., and Ly, H. 1995, *J. Am. Chem. Soc.*, 117, 12528.
35. Nazmutdinov, R. R., Zhang, J., Zinkicheva, T. T., Manyurov, I. R., and Ulstrup, J. 2006, *Langmuir*, 22, 7556.
36. Di Felice, R., Selloni, A., and Molinari, E. 2003, *J. Phys. Chem. B*, 107, 1151.
37. Di Felice, R. and Selloni, A. 2004, *J. Chem. Phys.*, 120, 4906.
38. Ihs, A. and Liedberg, B. 1991, *J. Colloid Interface Sci.*, 144, 282.
39. Uvdal, K., Bodö, P., and Liedberg, B. 1992, *J. Colloid Interface Sci.*, 149, 162.
40. Leggett, G. J., Davies, C. M., Jackson, D. E., and Tendler, S. J. B. 1993, *J. Phys. Chem.*, 97, 5348.
41. McDermott, C. A., McDermott, M. T., Green J. B., and Porter, M. D. 1995, *J. Phys. Chem.*, 99, 13257.
42. Cavalleri, O., Gonella, G., Terreni, S., Vignolo, M., Floreano, L., Morgante, A., Canepa, M., and Rolandi, R. 2004, *Phys. Chem. Chem. Phys.*, 6, 4042.
43. Cavalleri, O., Gonella, G., Terreni, S., Vignolo, M., Pelori, P., Floreano, L., Morgante, A., Canepa, M., and Rolandi, R. 2004, *J. Phys. : Condens. Matter*, 16, S2477.
44. Xu, Q. M., Wan, L. J., Wang, C., Bai, C. L., Wang, Z. Y., and Nozawa, T. 2001, *Langmuir*, 17, 6203.

- 
45. De Renzi, V., Lavagnino, L., Corradini, V., Biagi, R., Canepa, M., and del Pennino, U. 2008, *J. Phys. Chem.*, 112, 14439.
  46. Cossaro, A., Terreni, S., Cavalleri, O., Prato, M., Cvetko, D., Morgante, A., Floreano, L., and Canepa, M. 2006, *Langmuir*, 22, 11193.
  47. Kühnle, A., Molina, L. M., Linderoth, T. R., Hammer, B., and Besenbacher, F. 2004, *Phys. Rev. Lett.*, 93, 086101.
  48. Kühnle, A., Linderoth, T. R., and Besenbacher, F. 2006, *J. Am. Chem. Soc.*, 128, 1076.
  49. Kühnle, A., Linderoth, T. R., Hammer, B., and Besenbacher, F., 2002, *Nature*, 415, 891.
  50. Kühnle, A., Linderoth, T. R., and Besenbacher, F. 2003, *J. Am. Chem. Soc.*, 125, 14680.
  51. Kühnle, A. 2009, *Current Opinion in Colloid and Interface Science*, 14, 157.